有机化学 DOI: 10.6023/cjoc202301003 研究论文
Chinese Journal of Organic Chemistry ARTICLE

高选择性比率型荧光探针用于急性肺损伤中次氯酸的检测

丁炳辉[a] 韩少辉[a] 熊海青[a] 王本花[a] 左伯军*,[b] 宋相志*,[a]
([a]中南大学化学化工学院 长沙 410083)
([b]山东农药科学研究院 济南 250033)

摘要 检测急性肺损伤中过表达的次氯酸要求荧光探针具有很高的选择性. 合成了一种羟基萘香豆素探针 **NaphCou**, 可以高选择性比值型检测次氯酸, 响应速度快, 发射波长长(从绿色到红色变化), Stokes 位移大(从 107 nm 到 155 nm). 利用该荧光探针, 成功监测了脂多糖诱导急性肺损伤小鼠中次氯酸的浓度变化.

关键词 急性肺损伤; 次氯酸; 荧光探针; 比值型

A Highly Selective Ratiometric Fluorescent Probe for the Detection of Hypochlorite in Acute Lung Injury

Ding, Binghui[a] Han, Shaohui[a] Xiong, Haiqing[a] Wang, Benhua[a]
Zuo, Bojun*,[b] Song, Xiangzhi*,[a]
([a] *College of Chemistry & Chemical Engineering, Central South University, Changsha 410083*)
([b] *Shandong Academy of Pesticide Sciences, Jinan 250033*)

Abstract The fluorescent probe for the detection of overexpressed ClO^- in acute lung injury is required to have high selectivity against other reactive species. A hydroxybenzo[*g*]coumarin, **NaphCou**, was synthesized as a ratiometric fluorescent probe to detect ClO^- with ultra-high selectivity, a fast response, long-wavelength emissions (from green to red) and large Stokes shifts (from 107 nm to 155 nm). Using probe **NaphCou** as a fluorescence sensing tool, the lipopolysaccharide (LPS)-induced acute lung injury in mouse model was investigated by monitoring the hypochlorous acid concentration variation.

Keywords acute lung injury; hypochlorous acid; fluorescent probe; ratiometric measurement

1 Introduction

Recently, the sustained global outbreak of COVID-19 has been leading to many complications of lung disease, even respiratory distress syndrome and acute lung injury (ALI).[1] ALI is an acute, persistent syndrome of inflammatory response in the lungs that induces damage to the alveolar capillary lining and increased capillary permeability.[2] If ALI is left untreated, it can result in life-threatening health problems. ALI are mainly mediated by the inflammation-related burst of reactive oxygen species (ROS) in the cells including hypochlorite (ClO^-), hydroxyl radical (HO•), singlet oxygen ($^1O_2$), hydrogen peroxide (H_2O_2), peroxynitrite ($ONOO^-$) and so on.[3] Among them, ClO^- plays an important role in the development of inflammation in organism.[4] Over-released ClO^- in lungs may be considered as one of the markers of ALI. Therefore, accurate monitoring of ClO^- in cells is of great interest for the diagnosis and treatment of ALI.

Compared with off-on fluorescent probes, ratiometric fluorescent probes can overcome fluorescence self-quenching and background signal interference.[5] In the past two decades, ratiometric fluorescent probes have been emerged as useful tools for the visualization and detection of ClO^- *in vivo*.[6] Since there are different kinds of overexpressed ROS species in ALI, ClO^- fluorescent probes are required to have ultra-high selectivity against other ROS species. To date, most of ClO^- fluorescent probes were designed based on ClO^--triggered oxidation reactions, including breakage of double bonds and the oxidation of chalcogen atoms, which are often interfered by other ROS species.[7] To address this issue, there should be a highly selective ClO^--triggered reaction for the design of ClO^- fluorescent probes.

* Corresponding authors. E-mail: xzsong@csu.edu.cn; zuobj@sina.com
Received January 4, 2023; revised March 12, 2023; published online April 13, 2023.
Project supported by the National Natural Science Foundation of China (No. 22178395).
国家自然科学基金(No. 22178395)资助项目.

It is known that ClO^- can chlorinate phenols at *ortho*- and/or *para*-position with a high selectivity.[8] Due to the inductive effect of chlorine atom, the chlorinated phenol has lower pK_a than the corresponding unchlorinated one.[9] Herein, we employed ClO^--triggered chlorination reactions as the sensing mechanism to develop ClO^- fluorescent probes. First, the reaction mechanism was studied by the investigation of the optical responses of 7-hydroxycoumarin toward ClO^-. Then, we fused one more benzene ring to 7-hydroxycoumarin to design a hydroxybenzo[*g*]-coumarin, **NaphCou**, which was easily obtained in two steps with 2,7-dihydroxynaphthalene as a starting material (Scheme 1). Probe **NaphCou** displayed a fast, highly selective and ratiometric fluorescence response toward ClO^- with long-wavelength emissions, and was applied to successfully track intracellular ClO^- in living cells and zebrafish. Particularly, the ability of this probe to investigate ALI was successfully demonstrated. The proposed mechanism of 7-hydroxycoumarin and **NaphCou** towards ClO^- was displayed in Scheme 2.

2 Results and discussion

2.1 Spectral responses and sensing mechanism of 7-hydroxycoumarin towards ClO^-

Since 7-hydroxycoumarin is a widely used fluorescent dye for the construction of fluorescent probes, the optical response of 7-hydroxycoumarin towards ClO^- was investigated. 7-Hydroxycoumarin has an absorption peak at 330 nm with a shoulder at 375 nm in phosphate buffered saline (PBS) buffer (10.0 mmol/L, pH＝7.4, containing 50% EtOH). The treatment of the solution of 7-hydroxy-coumarin with ClO^- resulted in the disappearance of the absorption peak at 330 nm and the enhancement of the band at 375 nm. In aqueous solution with a certain pH value, the dissociation of OH group in 7-hydroxycoumarin makes it exist in phenol form and phenolate form. And the conversion equilibrium between the two forms depends on the pK_a of 7-hydroxycoumarin and pH of the media. The 330 nm absorption band should be assigned to the phenol form and the 375 nm band results from the phenolate form. Since 7-hydroxycoumarin has pK_a of 7.8, it mainly exists in its phenolate form in a pH＝7.4 PBS buffer (Scheme 2).[10] When the solution of 7-hydroxycoumarin was treated with ClO^-, 7-hydroxycoumarin was chlorinated to produce chlorinated 7-hydroxycoumarin which would exist in the phenolate form due to the decreased pK_a (Scheme 2). In order to prove the above hypothesis, NaOH solution was added into the solution of 7-hydroxycoumarin to observe the absorption spectral change. The addition of NaOH solution induced a ratiometric absorption change, and the final absorption spectrum is very similar to that of the mixture of 7-hydroxycoumarin with ClO^-. Furthermore, aqueous HCl solution was used to acidify the solution of 7-hydroxycoumarin or the mixture of 7-hydroxycoumarin with ClO^-, and only the phenol absorption band at 330 nm was seen.

Upon excited, 7-hydroxycoumarin displayed only one emission band at 452 nm. The addition of ClO^- only induced a 3-fold fluorescence enhancement with no spectral shift. The phenol form of 7-hydroxycoumarin was non-fluorescent, while the phenolate form was strongly fluorescent. In PBS buffer (pH＝7.4), the chlorinated 7-hydroxycoumarin mainly existed in the strongly fluorescent phenolate. A fluorescence enhancement was observed when 7-hydroxycoumarin was treated with NaOH solution and a similar fluorescence spectrum was obtained when 7-hydroxycoumarin was treated with either NaOH or

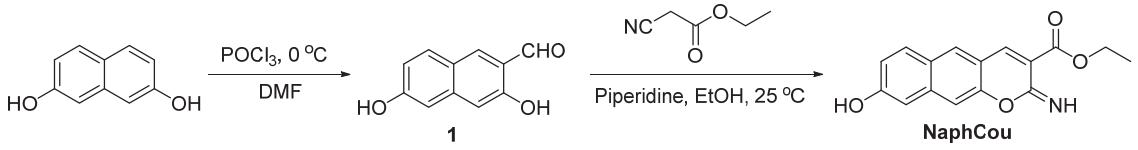

Scheme 1 Synthetic route of probe **NaphCou**

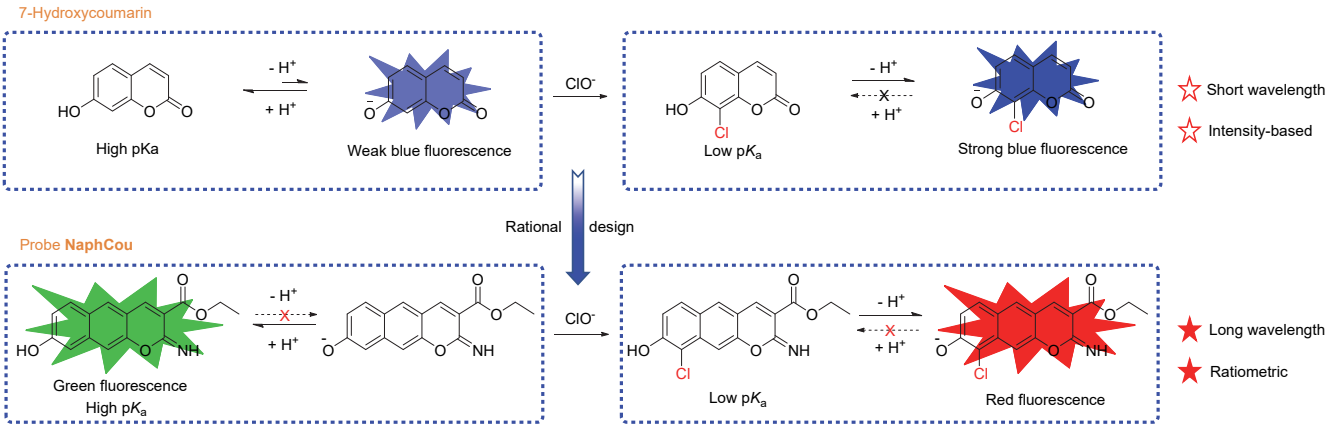

Scheme 2 Proposed sensing mechanism of 7-hydroxycoumarin and probe **NaphCou** towards ClO^- at pH 7.4

ClO^-. Furthermore, a drastic fluorescence quench was seen when 7-hydroxycoumarin or the mixture of 7-hydroxycoumarin and ClO^- was acidified with aqueous HCl solution. The concentration dependent fluorescence study of 7-hydroxycoumarin towards ClO^- was carried out. 7-Hydroxycoumarin could quantitatively detect ClO^- with a good linear relationship between the fluorescence intensity and the concentration of ClO^- (0～200.0 μmol/L). Given the strong initial fluorescence of 7-hydroxycoumarin, it could not be regarded as a good intensity-based fluorescent probe.

2.2 Design of ratiometric fluorescent probe **NaphCou**

Using the above sensing mechanism to develop a ratiometric fluorescent probe to detect ClO^-, it is required that both the fluorescent probe and its chlorinated analogue should be fluorescent with distinct signals and have different pK_a values striding across the physiological pH (7.4). To obtain such a probe, one more benzene ring was fused into 7-hydroxycoumarin to obtain a derivative of 8-hyroxybenzo[*g*]coumarin, **NaphCou**. **NaphCou** exhibits a longer emission wavelength due to its extended conjugation system than 7-hydroxycoumarin.[11] Moreover, it was expected that **NaphCou** and its chlorinated analogue (**NaphCou-Cl**) would own different pK_a values around physiological pH value, resulting in a ratiometric fluorescence signal to ClO^-. The proposed mechanism of **NaphCou** towards ClO^- was illustrated in Scheme 2.

2.3 Absorption and emission spectral studies of probe **NaphCou** towards ClO^-

As shown in Figure 1, the absorption maximum of probe **NaphCou** is around 400 nm and gives off a green emission with λ_{max}=507 nm. After addition of ClO^- into the solution of probe **NaphCou**, a red emission with λ_{max}=640 nm was observed. Noteworthy, the Stokes shifts of this probe were substantially large before and after the treatment with ClO^- (107 nm and 155 nm, respectively), which was desirable for the fluorescence sensing.

To investigate whether this probe can qualitatively determine ClO^-, a fluorescence titration experiment was carried out by measuring the ratio of the fluorescence intensity at 640 and 507 nm ($I_{640\ nm}/I_{507\ nm}$) with increasing the concentration of ClO^- (Figure 2). It was seen that the increase of the concentration of ClO^- resulted in a decrease of fluorescence signal at 507 nm and a concurrent increase of the fluorescence signal at 640 nm. The ratio of $I_{640\ nm}/I_{507\ nm}$ reached a plateau when 120.0 μmol/L ClO^- was added. There was a good linear relationship (R^2=0.995) between the ratio of $I_{640\ nm}/I_{507\ nm}$ and the concentration of ClO^- (0～100.0 μmol/L), and the detection limit (S/N=3) was determined to be 11.6 nmol/L.

Subsequently, the response time between probe **NaphCou** and ClO^- was investigated by determining the ratio of $I_{640\ nm}/I_{507\ nm}$ as a function of time after addition of different concentrations of ClO^- to the solution of probe **NaphCou** (10.0 μmol/L). As evident from Figure 3, the ratio of $I_{640\ nm}/I_{507\ nm}$ increased within seconds after the adding ClO^-. Upon adding 4.0, 8.0, and 12.0 equiv. of ClO^-, the equilibrium could be reached within 6, 12 and 18 s with the 2.5, 5.8, and 8.3-fold enhancements in the ratio of $I_{640\ nm}/I_{507\ nm}$, respectively. The results indicated that this probe had a rapid response to ClO^- and its potential applicability for real-time imaging in the field of biology.

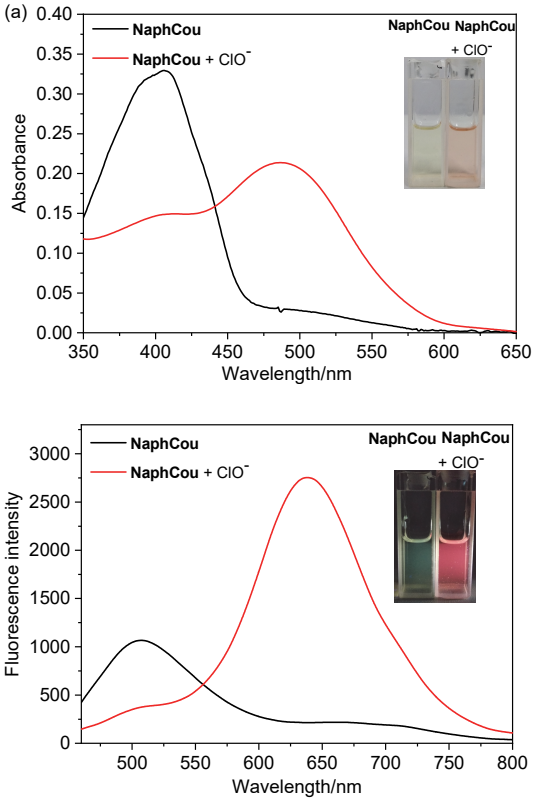

Figure 1 Absorption (a) and emission (b) spectra of probe **NaphCou** (10.0 μmol/L) without (black line) and with (red line) of ClO^- (120.0 μmol/L)

Insets: color (a) and fluorescence (b) images of probe **NaphCou** (10.0 μmol/L) with/without of ClO^- (120.0 μmol/L).

2.4 Selectivity studies of probe **NaphCou** towards ClO^-

In order to evaluate the selectivity of probe **NaphCou**, the fluorescence responses of probe **NaphCou** towards common reactive oxygen species were investigated, reactive oxygen species including ClO^-, HO•, $^1O_2$, H_2O_2, KO_2, NO•, $ONOO^-$, ROO•, TBHP, *t*-BuO•, O_2^-, BrO^-, H_2S and SO_2. As seen in Figure 4, all the interfering species caused negligible fluorescence change except for ClO^-. In addition, the co-existence of other reactive oxygen species had little impact on the performance of probe **NaphCou**. These results clearly suggested that probe **NaphCou** was highly selective for ClO^-.

2.5 pH effect on the performance of probe **NaphCou** towards ClO^-

To optimize the operating condition, the performance of probe **NaphCou** to detect ClO^- under different pH values

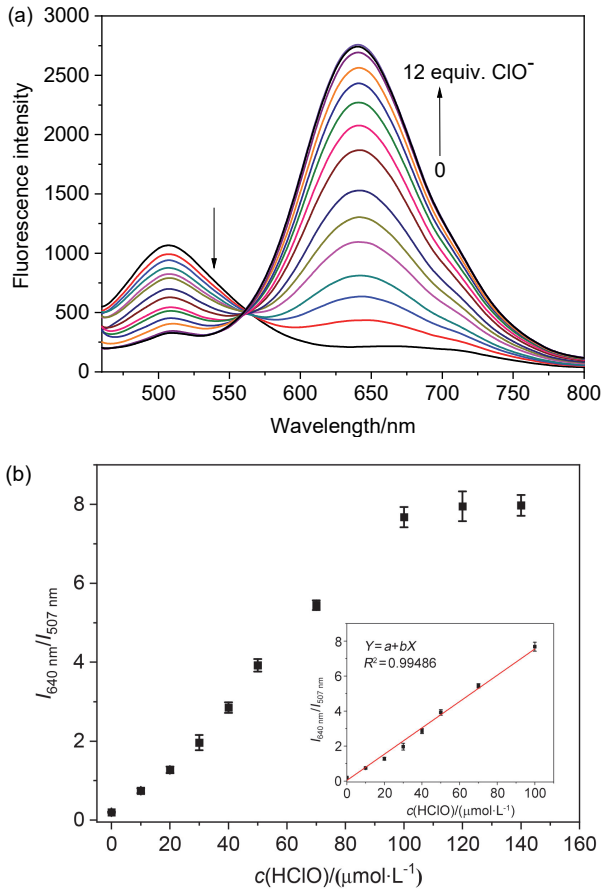

Figure 2 Emission spectra (a) and the fluorescence intensity ratio ($I_{640\ nm}/I_{507\ nm}$) (b) of probe **NaphCou** (10.0 μmol/L) with ClO^- (0～12 equiv.) and parallel tests 3 times

Inset: the linear relationship between the ratio of $I_{640\ nm}/I_{507\ nm}$ and the concentration of ClO^-

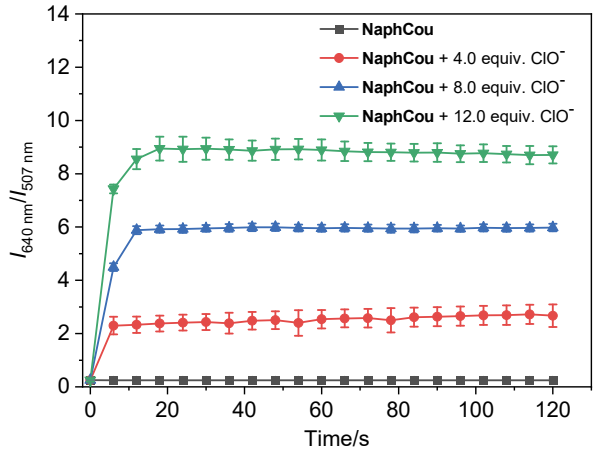

Figure 3 Ratio of $I_{640\ nm}/I_{507\ nm}$ *vs* time after 4.0, 8.0 and 12.0 equiv. of ClO^- were added into the solution of probe **NaphCou**

was investigated. The ratio of $I_{640\ nm}/I_{507\ nm}$ was large when the solution of probe **NaphCou** was treated with ClO^- between pH 7.0 and 10.0. In contrast, the ratio of $I_{640\ nm}/I_{507\ nm}$ of probe **NaphCou** showed little change in the absence of ClO^- within a pH range of 2.0～10.0. These experimental results indicated that probe **NaphCou** could work under the physiological condition.

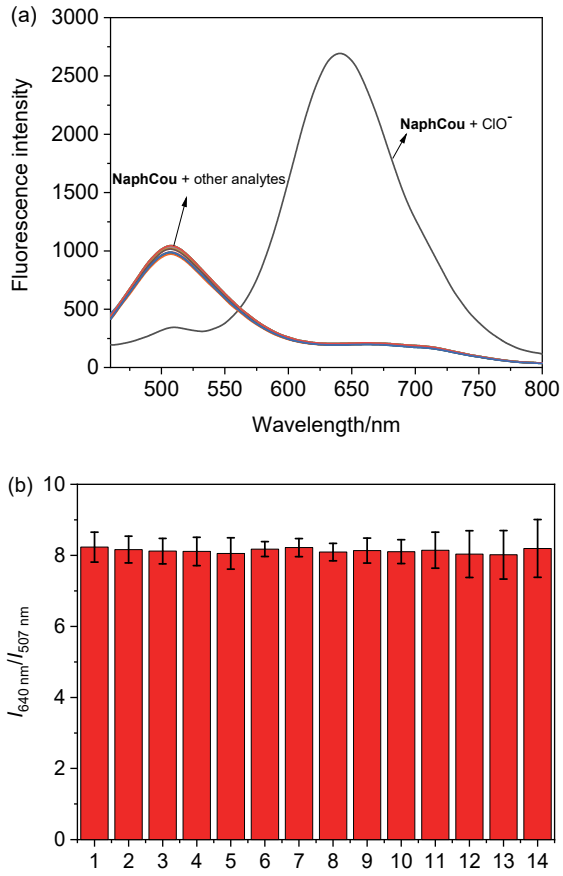

Figure 4 (a) Emission spectra of probe **NaphCou** (10.0 μmol/L) with various interferential analytes. (b) The ratio of $I_{640\ nm}/I_{507\ nm}$ of probe **NaphCou** (10.0 μmol/L) in response to ClO^- in the presence of other interfering analytes

1, blank; 2, HO•; 3, $^1O_2$; 4, H_2O_2; 5, KO_2; 6, NO•; 7, $ONOO^-$; 8, ROO•; 9, TBHP; 10, *t*-BuO•; 11, O_2^-; 12, BrO^-; 13, H_2S; 14, SO_2.

2.6 Sensing mechanism of probe **NaphCou** towards ClO^-

The proposed sensing mechanism of probe **NaphCou** towards ClO^- is shown in Scheme 2. To support the mechanism, **NaphCou-Cl** was also synthesized, and its optical properties were investigated. It was observed that **NaphCou-Cl** and the mixture of probe **NaphCou** with ClO^- had nearly identical absorption and emission spectra. Furthermore, HRMS spectral analysis on the mixture of probe **NaphCou** and ClO^- showed there was a peak at 316.0388, corresponding to the molecular weight of **NaphCou-Cl** ($[M-H]^-=316.0382$). Probe **NaphCou** predominantly exists in the phenol form, whereas **NaphCou-Cl** completely exists in the phenolate form at pH 7.4 because **NaphCou-Cl** would have a lower pK_a values. Consequently, **NaphCou-Cl** displays a red-shifted fluorescence at pH 7.4 due to the enhanced ICT effect.

2.7 Ratiometric imaging of ClO^- in living cells and zebrafish

The high sensitivity and good selectivity of probe **NaphCou** for ClO^- in solution encouraged us to explore

its application in biological samples. In Figure 5, the R/G value increased from 0.02 to 19.0 from the control group to the experimental group, in Figures 6 and 7, this value ranged from 0.05 to 20.5 and from 0.28 to 3.90, respectively, which proves that probe **NaphCou** has good ability ratiometric detection of hypochlorous acid in biological samples. The MTT (3-[4,5-dimethylthiazol-2-yl]-2,5 diphenyl tetrazolium bromide) assay was first investigated on A549 cells. The cell viability was over 90% when A549 cells were treated with 20.0 μmol/L of probe **NaphCou** for 24 h, which proved probe **NaphCou** is low toxicity. Then, the ability of probe **NaphCou** to detect ClO^- in living A549 cells was evaluated. When cells were incubated with probe **NaphCou** (10.0 μmol/L) for 30 min, only green fluorescence signals were observed. In contrast, cells treated with ClO^- (120.0 μmol/L) and probe **NaphCou** (10.0 μmol/L) successively only displayed a bright red fluorescence (Figure 5). In addition, the fluorescence imaging of probe **NaphCou** in three-day-old zebrafish under the same condition in A549 cells was investigated. As displayed in Figure 6, the imaging results were also proved that probe **NaphCou** could be effectively used to ratiometric image ClO^- in zebrafish.

2.8 Ratiometric imaging of ClO^- in acute lung injury (ALI) of mice model

ClO^- is overexpressed in acute lung injury of mice. The lipopolysaccharide (LPS) was used to induced ALI of mice. Then, the lung tissue from normal mice and ALI mice was dissected and sectioned into 10 μm slides. The success of LPS-induces ALI was confirmed by H&E staining. Compared to the normal group, LPS-induced mice showed significant alveolar damage and inflammatory response with marked inflammatory cell infiltration (Figure 7). Finally, the lung slides were treated with probe **NaphCou** (10 μmol/L) for 30 min. In the lung slides of normal mice, strong fluorescence signals only gave off from the green channel. Distinctly, bright red fluorescence and essentially no green fluorescence were detected in the lung slides of ALI mouse (Figure 7A).

3 Conclusions

In summary, a ratiometric fluorescent probe was developed for the detection of ClO^- in acute lung injury with

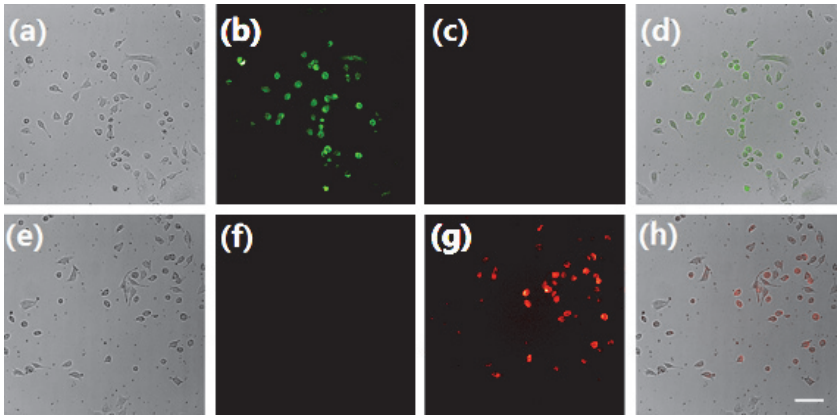

Figure 5 Bright (the first column), fluorescence (the second and third columns) and merged (the fourth column) images of A549 cells
Top row: cells incubated with probe **NaphCou** (10.0 μmol/L) for 30 min; bottom row: cells treated with ClO^- (120.0 μmol/L) for 30 min and then incubated with probe **NaphCou** (10.0 μmol/L) for 30 min. Emission was collected at 490～520 nm for the green channel and 620～650 nm for the red channel. λ_{ex}=435～460 nm. Scale bar=50 μm.

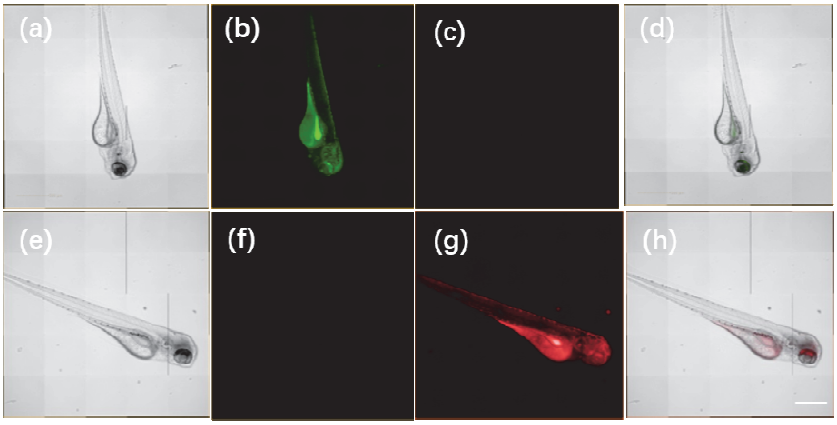

Figure 6 Bright (the first column), fluorescence (the second and third columns) and merged (the fourth column) images and of zebrafish
Top row: zebrafish incubated with probe **NaphCou** (10.0 μmol/L) for 30 min; bottom row: zebrafish treated with ClO^- (120.0 μmol/L) for 30 min and then incubated with probe **NaphCou** (10.0 μmol/L) for 30 min. Emission was collect at 490～520 nm for the green channel and 620～650 nm for the red channel. λ_{ex}=435～460 nm. Scale bar=200 μm.

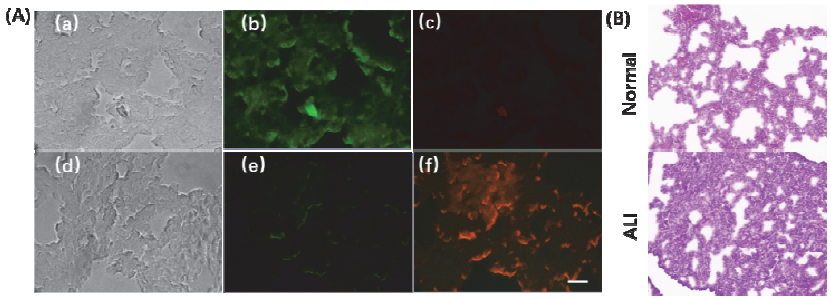

Figure 7 (A) Bright (the first column) and fluorescence (the second and third columns) images of lung histology slides of the normal (a～c) and ALI (d～f) mice treated with probe **NaphCou** (10.0 μmol/L) for 30 min. (B) Pathological changes of the lung tissue of normal and ALI mice (H&E staining)

Scale bar＝200 μm.

high selectivity to avoid interference from the other reactive oxygen species. Based on the ClO^--triggered chlorination reaction on phenol, probe **NaphCou** was designed and synthesized to detect ClO^- with high sensitivity, a fast response, long-wavelength emissions. Further, probe **NaphCou** was demonstrated in the ratiometric imaging ClO^- in living cells, zebrafish, and acute lung injury of mice model, which suggested that it has great potential to investigate the state of acute lung injury in clinic.

4 Experimental section

4.1 Instruments and reagents

^1H NMR and ^{13}C NMR spectra were obtained using a Bruker 400 spectrometer. The mass spectra were obtained using a Bruker Daltonics micr-OTOF-Q II spectrometer. Emission spectra were recorded on a Hitachi F-7000 fluorometer, and UV-vis absorption spectra were recorded on a Shimadzu UV-2450 spectrophotometer. A Leici PHS-3C pH meter was used for pH measurements. Fluorescence imaging experiments were conducted using an Opera Phenix/Operetta CLS system from PerkinElmer and an Olympus IX83 inverted microscope. A549 cells and zebrafish were obtained from Xiangya Hospital at Central South University and Nanjing Eze-Rinka Biotechnology Co., Ltd. China, respectively. For the study in the LPS-induced acute lung injury, lung histology slides of mouse were purchased from Wuhan Servicebio Technology Co., Ltd., China. All the chemicals were purchased form the commercial suppliers and used without further purification.

4.2 Spectral measurements

Each bar in this paper represents the mean±SD of three experiments. Unless otherwise specified, spectra of 7-hydroxycoumarin and probe **NaphCou** towards ClO^- were investigated in PBS buffer (10.0 mmol/L, pH＝7.4, containing 50% EtOH). Excitation wavelength: 372 nm for 7-hydroxycoumarin with ClO^- and 440 nm for probe **NaphCou** with ClO^-.

4.3 Synthesis

4.3.1 Synthesis of compound **1**

2,7-Dihydroxynaphthalene (7.5 mmol, 1.2 g) was dissolved in 10 mL of dry *N*,*N*-dimethylformamide (DMF). After being stirred at 0 ℃ for 30 min, $POCl_3$ (11.2 mmol, 1.7 g) was added to the mixture dropwise. The reaction mixture solidified within 30 min. Then, added 20 mL of water to the reaction mixture, and stirred with a glass rod and sonicated for 10 min. The mixture was filtrated, and the obtained filtrate was stood for 2 h at room temperature to precipitate out a large amount of yellow solid. The solid was collected by filtration and washed with water to give pure compound **1** (390 mg, yield 24%). Yellow solid, m.p. 166～168 ℃; ^1H NMR (400 MHz, DMSO-d_6) δ: 11.73 (s, 1H), 10.70 (s, 1H), 9.99 (s, 1H), 8.32 (s, 1H), 7.96 (d, J＝8.9 Hz, 1H), 7.70 (d, J＝8.8 Hz, 1H), 6.95 (d, J＝8.9 Hz, 2H); ^{13}C NMR (100 MHz, DMSO-d_6) δ: 192.4, 165.1, 159.4, 138.8, 134.2, 131.1, 122.7, 116.3, 115.1, 112.1, 105.7; HRMS (ESI) calcd for $C_{11}H_8NaO_3$ $[M+Na]^+$ 211.0366, found 211.0369.

4.3.2 Synthesis of **NaphCou**

To a solution of compound **1** (0.5 mmol, 94 mg) and ethyl cyanoacetate (0.6 mmol, 68 mg) in 2 mL of anhydrous ethanol was added 50 μL of piperidine. The resulting mixture was stirred at 25 ℃ for 2 h and a yellow solid was precipitated out. The solid was collected by filtration and washed with ethanol to give pure **NaphCou** (105 mg, yield 74%). Yellow solid, m.p. 282～284 ℃; ^1H NMR (400 MHz, DMSO-d_6) δ: 10.24 (s, 1H), 9.25 (s, 1H), 8.69 (s, 1H), 8.06 (d, J＝8.8 Hz, 1H), 7.85 (d, J＝8.8 Hz, 1H), 7.54 (s, 1H), 7.14 (dd, J＝22.8, 8.8 Hz, 2H), 4.36 (q, J＝7.0 Hz, 2H), 1.38 (t, J＝7.1 Hz, 3H); ^{13}C NMR (100 MHz, DMSO-d_6) δ: 164.7, 158.9, 155.3, 136.2, 131.9, 131.4, 124.4, 118.2, 113.1, 109.9, 104.1, 61.9, 14.5; HRMS (ESI) calcd for $C_{16}H_{12}NO_4$ $[M-H]^-$ 282.0766, found 282.0752.

Supporting Information The synthesis of **NaphCou-Cl**, additional optical spectra, ^1H NMR and ^{13}C NMR spectra, HRMS spectra and biological experiments of 7-hydroxycoumarin, **NaphCou** and **NaphCou-Cl**. The Supporting Information is available free of charge via the Internet at http://sioc-journal.cn/.

References

[1] (a) Mitchell, W. B. *Paediatr. Respir. Rev.* **2020**, *35*, 20.

(b) Gallelli, L.; Zhang, L. M.; Wang, T.; Fu, F. H. *J. Clin. Pharmacol.* **2020**, *60*, 815.
[2] (a) Mowery, N. T.; Terzian, W. T. H.; Nelson, A. C. *Curr. Prob. Surg.* **2020**, *57*, 100777.
(b) Cheung, O. Y.; Graziano, P.; Leslie, K. O. *Practical Pulmonary Pathology*: *A Diagnostic Approach (Second Edition)*, Ed.: Saunders, W. B., Philadelphia, **2011**, pp. 117～136.
[3] (a) Kellner, M.; Noonepalle, S.; Lu, Q.; Srivastava, A.; Zemskov, E.; Black, S. M. *Adv. Exp. Med. Biol.* **2017**, *967*, 105.
(b) Schieber, M.; Chandel, N. S. *Curr. Biol.* **2014**, *24*, 453.
[4] (a) Pattison, D. I.; Davies, M. J. *Biochemistry* **2004**, *43*, 4799.
(b) Fukuyama, T.; Martel, B. C.; Linder, K. E.; Ehling, S.; Ganchingco, J. R.; Bäumer, W. *Clin. Exp. Allergy* **2018**, *48*, 78.
(c) Rayner, B. S.; Zhang, Y. J.; Brown, B. E.; Reyes, L.; Cogger, V. C.; Hawkins, C. L. *Free Radic. Biol. Med.* **2018**, *129*, 25.
[5] (a) Qin, T. Y.; Zhao, X. F.; Song, C.; Chen, S. H.; Xu, Z. Y.; Zhang, Z. X.; Lv, T. Y. Z.; Xun, Z. Q.; Liu, B.; Peng, X. J. *Chem. Eng. J.* **2023**, *451*, 139022.
(b) Luo, Z. J.; Lv, T. Y. Z.; Zhu, K. N.; Li, Y.; Wang, L.; Gooding, J. J.; Liu, G. Z.; Liu, B. *Angew. Chem., Int. Ed.* **2020**, *59*, 3131.
[6] Zhao, Y.; Li, Y. F.; Li, R. X.; Wang, Y. Q.; Fan, X. X. *Chin. J. Org. Chem.* **2021**, *41*, 1974 (in Chinese).
(赵云, 李艳芳, 李蓉晓, 王雅卿, 樊晓霞, 有机化学, **2021**, *41*, 1974.)
[7] (a) Yue, X. X.; Wang, J. P.; Han, J. L.; Wang, B. H.; Song, X. Z. *Chem. Commun.* **2020**, *56*, 2849.
(b) Zang, S. P.; Kong, X. X.; Cui, J.; Su, S.; Shu, W.; Jing, J.; Zhang, X. L. *J. Mater. Chem. B* **2020**, *8*, 2660.
(c) Zhang, Y.; Yang, H. Y.; Li, M. X.; Gong, S.; Song, J.; Wang, Z. L.; Wang, S. F. *Dyes Pigm.* **2022**, *197*, 109861.
(d) Liang, L. J.; Sun, Y. M.; Liu, C.; Zeng, X. S.; Zhao, J. L. *Dyes Pigm.* **2021**, *190*, 109344.
(e) Chen, Y.; Lim, J. Y.; Wu, X. H.; Heo, J. S.; Yuan, F. Y.; Zhang, J. F.; Yoon, D. W.; Ren, W. X. *Dyes Pigm*. **2021**, *195*, 109666.
(f) Han, J. L.; Yang, S.; Wang, B. H.; Song, X. Z. *Anal. Chem.* **2021**, *93*, 5194.
(g) Lamb, B. M.; Barbas Iii, C. F. *Chem. Commun.* **2015**, *51*, 3196.
(h) Xu, Q. L.; Lee, K. A.; Lee, S.; Lee, K. M.; Lee, W. J.; Yoon, J. *J. Am. Chem. Soc.* **2013**, *135*, 9944.
(i) Xiao, H. D.; Li, J. H.; Zhao, J.; Yin, G.; Quan, Y. W.; Wang, J.; Wang, R. Y. *J. Mater. Chem. B* **2015**, *3*, 1633.
(j) Wu, M. Y.; He, T.; Li, K.; Wu, M. B.; Huang, Z.; Yu, X. Q. *Analyst* **2013**, *138*, 3018.
(k) Han, J. L.; Liu, X. J.; Xiong, H. Q.; Wang, J. P.; Wang, B. H.; Song, X. Z.; Wang, W. *Anal. Chem.* **2020**, *92*, 5134.
(l) Shen, Y. M.; Liu, X.; Zhang, X. Y.; Zhang, Y. Y.; Gu, B. *Spectrochim. Acta*, *Part A* **2020**, *239*, 118515.
(m) Mao, Z. Q.; Ye, M. T.; Hu, W.; Ye, X. X.; Wang, Y. Y.; Zhang, H. J.; Li, C. Y.; Liu, Z. H. *Chem. Sci.* **2018**, *9*, 6035.
(n) Xia, Q. N.; Wang, X. Y.; Liu, Y. N.; Shen, Z. F.; Ge, Z. G.; Huang, H.; Li, X.; Wang, Y. G. *Spectrochim. Acta*, *Part A* **2020**, *229*, 117992.
(o) Zhang, J.; Kan, J. F.; Sun, Y. Y.; Won, M.; Kim, J. H.; Zhang, W. F.; Zhou, J.; Qian, Z. S.; Kim, J. S. *ACS Appl. Bio Mater.* **2021**, *4*, 2080.
[8] Ge, F.; Zhu, L. Z.; Chen, H. R. *J. Hazard. Mater.* **2006**, *133*, 99.
[9] Liptak, M. D.; Gross, K. C.; Seybold, P. G.; Feldgus, S.; Shields, G. C. *J. Am. Chem. Soc.* **2002**, *124*, 6421.
[10] Moriya, T. *Bull. Chem. Soc. Jpn.* **1988**, *61*, 1873.
[11] Sarkar, S.; Santra, M.; Singha, S.; Jun, Y. W.; Reo, Y. J.; Kim, H. R.; Ahn, K. H. *J. Mater. Chem. B* **2018**, *6*, 4446.

(Cheng, F.)

